

Effect of Applied Potential and Sulfate Reducing Bacteria on Corrosion Behavior of X80 Steel in Dagang Soil Simulated Solution

Xiaoqing Sun, Fei Xie, Dan Wang, Ji Qi*

Key Laboratory of Oil & Gas Storage and Transportation, College of Petroleum Engineering, Liaoning Shihua University, Fushun Liaoning, 113001, China.

*E-mail: xiefei0413@163.com

Received: 3 February 2020 / *Accepted:* 31 March 2020 / *Published:* 10 May 2020

The corrosion behavior of X80 steel in Dagang soil simulated solution was verified by potentiostatic immersion test and AC impedance test, and the corrosion morphology of metal surface under different applied potential in bacterial solution and sterile solution was observed by scanning electron microscope (SEM). The results showed that the existence of sulfate reducing bacteria (SRB) can increase the corrosion trend of metals. In the simulated solution, the corrosion of samples became more and more serious with the increase of soaking days. With the negative shift of applied potential, the electrochemical corrosion rate of X80 pipeline steel was lower than that under self-corrosion potential.

Keywords: applied potential, SRB, X80 pipeline steel, AC impedance test

1. INTRODUCTION

X80 steel is widely used in West-to-East Gas Transmission Line 2 and other pipeline projects because of its high strength and good toughness.[1] X80 steel has also been put into practical application abroad. The successful construction of the second West-to-East Gas Transmission Line proves that the application of China's X80 pipeline steel and pipeline technology have been among the advanced ranks in the world in some aspects.[2]The heavy use of the oil and gas pipelines has drawn people's attention to its safe operation. Due to the particularity of buried environment, soil will corrode the oil field gathering pipeline. According to statistics, the annual loss caused by corrosion in China was as high as 2 trillion yuan, which accounts for about 3.34% of the total GDP in 2014.[3]Many studies had found that because the soil contains water and air, an electrolyte conductor is formed, which can cause corrosion by electrochemical reaction with the gathering pipeline. In addition, there is oxygen in the soil, so it is easy to form oxygen concentration cell, which greatly accelerates the corrosion behavior of oil

gathering pipelines. Pipeline corrosion behavior will also be affected by many other factors, such as microorganisms, applied potential, soil pH value, salt content, resistivity and so on.

Microbial corrosion refers to metal corrosion related to the action of microorganisms in the corrosion system. Microbes often exist in the soil or seabed where pipes are buried. 50% of the faults in buried pipelines come from microbial corrosion (mainly sulfate reduction process).[4]Worldwide, the loss caused by microorganisms involved in corrosion process is as high as hundreds of billions of dollars.[5]Among them, sulfate reducing bacteria (SRB) is the main cause of microbial corrosion in soil.[6-7]At present, the research on SRB-induced metal corrosion by many scholars at home and abroad is mainly focused on the mechanism of electrochemical corrosion.Miranda et al. believed that SRB can use the organic matter adsorbed on the metal surface as a carbon source to reduce sulfate to hydrogen sulfide and sulfide, resulting in increased metal corrosion. [8-9] Booth and others argued that SRB consumes cathode hydrogen through the action of hydrogenase,thus accelerating metal corrosion. [10-11] The above researches have not clearly demonstrated the relationship between SRB and metal corrosion behavior, especially for the corrosion behavior of high strength pipeline steel in the actual soil environment with SRB has not been reported. Therefore, it is necessary to further study the influence of microorganisms on pipeline corrosion behavior.

In the terms of applied potential, there is an electrochemical reaction in the corrosion process of pipeline steel, so the degree of corrosion will affect the electrochemical behavior of the electrode with or without applied potential. At present, scholars at home and abroad mainly focus on the effect of applied potential on stress corrosion cracking behavior of pipeline steel. Liu studied the SCC mechanism of pipeline steel in near neutral pH solution under cathodic protection (CP). The results showed that in the state of cathodic polarization there is a critical potential range (-730 ~ -920 mV). In this potential range, the crack tip of pipeline steel is in an unsteady electrochemical state, and there is a possibility of anodic dissolution (AD). When the polarization potential is higher than the critical range, SCC is the AD mechanism and when the polarization potential is lower than the critical range, SCC is hydrogen embrittlement (HE) mechanism. When the polarization potential is within the critical range, SCC is a mix mechanism of AD and HE.[12-13]However, the above research results lack the confirmation of the results of crack propagation test and crack tip electrochemical test.In addition, the corrosion behavior of X80 steel was studied mainly under the background of simulated $\text{NaHCO}_3+\text{Na}_2\text{CO}_3$ solution with high pH value, NS_4 solution simulating near neutral pH value, and soil simulation solution from typical soil corrosion test stations in China.[14-15][16-17][18-19]However, there are few reports about the effect of applied potential on corrosion behavior of high strength pipeline steel.

There are many influencing factors of pipeline corrosion, and its mechanism is too complex to be understood deeply.Although the research on the effect of microbial corrosion on pipeline corrosion behavior and the effect of applied potential on pipeline corrosion behavior has been in progress, the research on the corrosion behavior of high strength pipeline steel under the synergistic action of SRB and applied potential has not been reported.

Dagang is located in the southeast of Tianjin and faces Bohai Bay to the east. Due to the needs of the development and production of Dagang oil field, a large number of oil and gas pipelines have been buried underground. Most of the land in this area is the beach of Bohai Sea, and the soil has a high salt content,which is a typical coastal saline soil and has strong corrosiveness to metal

materials.[20]Therefore, it is of great significance to strengthen the study on the corrosion behavior of X80 pipeline steel in Dagang soil environment. In this work, under laboratory conditions, the corrosion behavior of X80 pipeline steel in bacterial and sterile solutions with or without applied potential was studied in Dagang soil simulated solution. In order to provide some reference and accumulate data for the corrosion protection of X80 pipeline steel in Dagang soil.

2. EXPERIMENTAL DETAILS

2.1 Experimental materials

The material used in the experiment is domestic X80 steel, which is a kind of acicular ferritic pipeline steel with high strength and toughness. The sample material is provided by the second West-to-East Gas Transmission line. Its chemical composition is shown in the table 1.1 below. The X80 steel was cut into electrochemical samples with the shape size of 1cm×1cm×2mm. During welding, a small amount of phosphoric acid was first stained, and then the wire was welded to the back of the working face of the sample with liquid tin, leaving the working area of the specimen as 1cm², and the rest was sealed in PTFE with epoxy resin. After the resin around the sample was solidified, the X80 steel working face was polished step by step in one direction with 360#, 800#, 1500# and 2000# of sandpaper, then washed with anhydrous ethanol and deionized water, removed oil from acetone and dried by cold air for later use.

Table 1. Chemical composition of X80 pipeline steel (wt %)

The quality of	C	Si	Mn	P	S	Cr	Ni	Ti	Nb	V	Mo
Mass fraction %	0.063	0.28	1.83	0.011	0.0006	0.03	0.03	0.016	0.061	0.059	0.22

2.2 Experimental method

The electrochemical experiment used three-electrode system, X80 steel sample as working electrode, platinum sheet as auxiliary electrode and saturated calomel electrode (SCE) as reference electrode. The schematic diagram of the specific device is shown in Figure 1. The setting time of open circuit potential was 3600s. The measurement of AC impedance was carried out on PARSTAT2273 electrochemical workstation. The measured frequency range was 10mHz~100kHz. The impedance spectrum was plotted by OriginPro8.5. The equivalent circuit of the test results of impedance spectrum was fitted and analyzed by ZSimDemo software, and the values of related components were recorded.

After the end of the experiment, the corrosion morphology of the surface layer of the specimen was observed by metallographic microscope. All the tests in this experiment were carried out at room temperature of 25°C, and the electrode potential was relative to SCE. In order to ensure the accuracy of

the data, three average experiments were carried out in all experiments, and the repeatability of data is good.

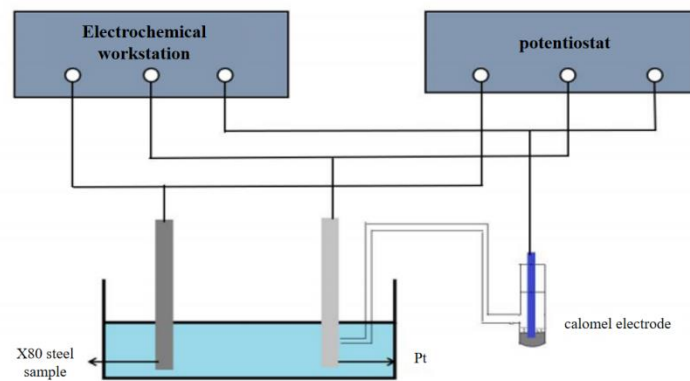


Figure 1. Schematic diagram of test equipment

3. RESULTS AND DISCUSSION

3.1 AC impedance test

The impedance spectrum of X80 steel samples in Dagang bacterial and sterile simulated solutions at -800mv potential is shown in Figure 2. To a certain extent, the size of the capacitive arc can reflect the difficulty of electrochemical corrosion of metals.

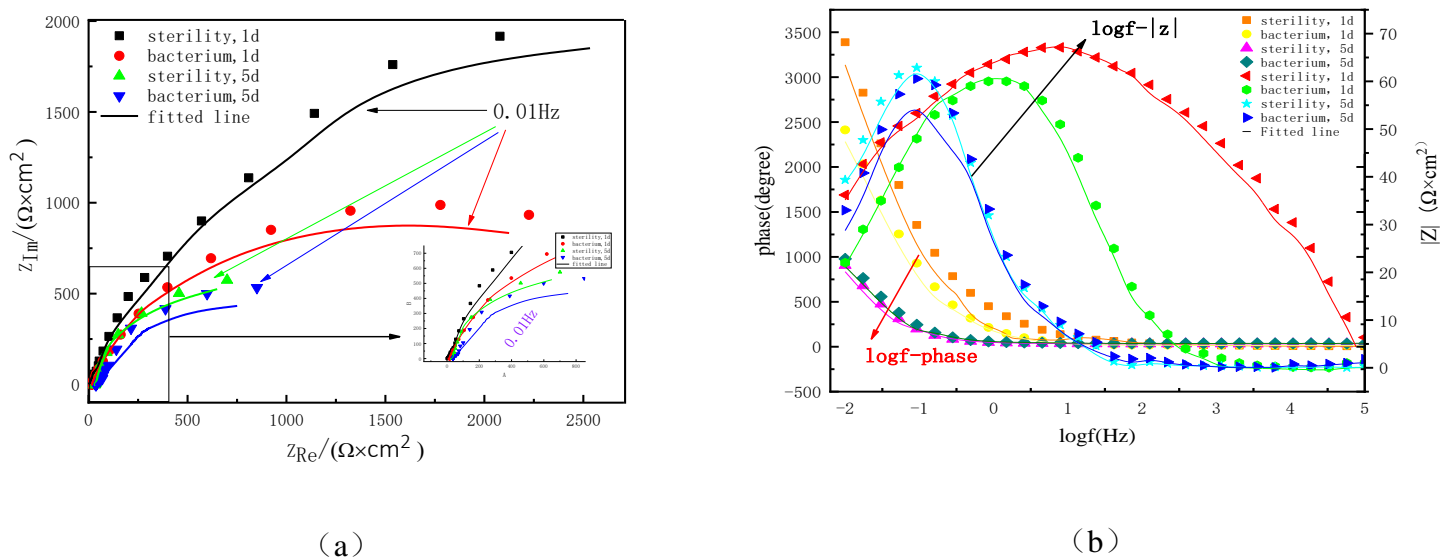


Figure 2. Electrochemical impedance spectroscopy of X80 steel in Dagang soil simulated solution under the bacterial and sterile conditions at -800mV potential (a) Nyquist diagram (b) Bode diagram

The larger the radius of the capacitive arc is, the greater the resistance to electrochemical corrosion of metals, and the slower the electrochemical corrosion rate of metals.[21]As can be seen from

Figure 2 (a), at the same immersion time, the measured capacitive arc radius of the sample in the bacterial solution was smaller than that in the sterile solution, which indicates that the existence of SRB bacteria could reduce the resistance of the corrosion reaction process. In the simulated solution of Dagang with bacteria, the capacitive arc radius of the sample soaked for 5 days was smaller than that of immersed for 1 day, which indicates that the sample was more prone to electrochemical corrosion at this time. As can be seen from Figure 2 (b), the Bode diagram of X80 steel had only one phase angle peak in the intermediate frequency region, which indicates that there was only one time constant in the electrode reaction process.

The equivalent circuit $R(C(R(CR)))$ was used to fit the AC impedance diagram, and the fitting circuit diagram is shown in Figure 3. And the $R_p = R_t + R_f$. As can be seen from the diagram, the experimental data was in good agreement with the fitting curve. C_{dl} represents electric double layer capacitance, R_s represents the solution resistance in the reaction process, R_t represents the charge transfer resistance in the reaction process, R_f represents the film resistance of the corrosion products generated, and R_p represents the polarization resistance in the whole reaction process, defining $R_p = R_t + R_f$. The polarization resistance can represent the resistance of the electrochemical reaction. The R_{p-1} is proportional to the corrosion rate of the metal. The higher the R_{p-1} , the faster the corrosion rate of the metal. [22] The change of R_p value under different conditions of -800mV potential is shown in Figure 4. It can be seen that for the sample soaked in sterile environment for 1 day had the highest R_p value, indicating the best corrosion resistance. For the sample soaked in the simulated solution with SRB for 5 days, the fitted R_p value was the lowest, indicating that the electrochemical corrosion rate of X80 steel was the highest at this time. R_p value changes as follows: bacterium 5d < sterility 5d < bacterium 1d < sterility 1d.

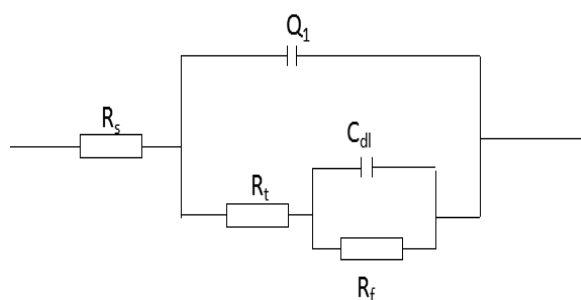


Figure 3. Equivalent circuit model of X80 steel in Dagang soil simulated solution under the bacterial and sterile conditions at -800mV potential

The impedance spectrum of X80 steel samples in Dagang bacterial and sterile simulated solutions without applied potential is shown in Figure 5. As shown in Figure 5 (a), it is close to the image shown in the case of applied potential, the measured impedance diagrams show the characteristics of a single capacitance arc. And at the same soaking time, the capacitive arc measured in the simulated solution with SRB was smaller than that in sterile simulated solution, indicating that the biofilm could reduce the corrosion resistance of X80 pipeline steel in Dagang soil simulated solution.

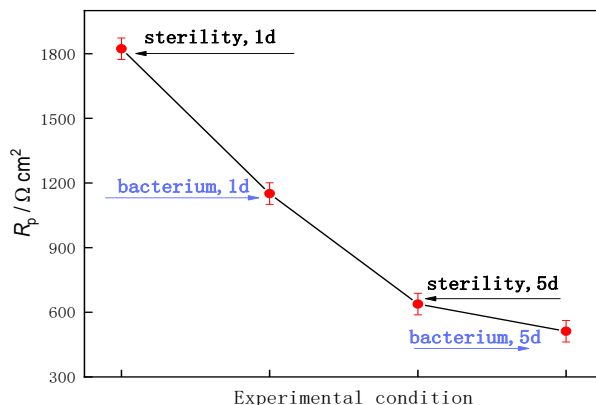


Figure 4. Variation of R_p value of X80 steel in Dagang soil simulated solution under the bacterial and sterile conditions at -800mV potential

As can be seen from Figure 5 (b), in Dagang simulated solution with bacteria, the capacitive arc radius of the sample soaked for 5 days was smaller than that of immersed for 1 day, which indicates that the sample was more prone to electrochemical corrosion at this time. The above law is consistent with the experimental law with applied potential, but the overall comparison shows that under the same conditions, the radius of capacitive reactance arc in the environment with -800mV potential is larger than that in the environment without applied potential, indicating that the applied potential can inhibit the corrosion reaction to a certain extent.

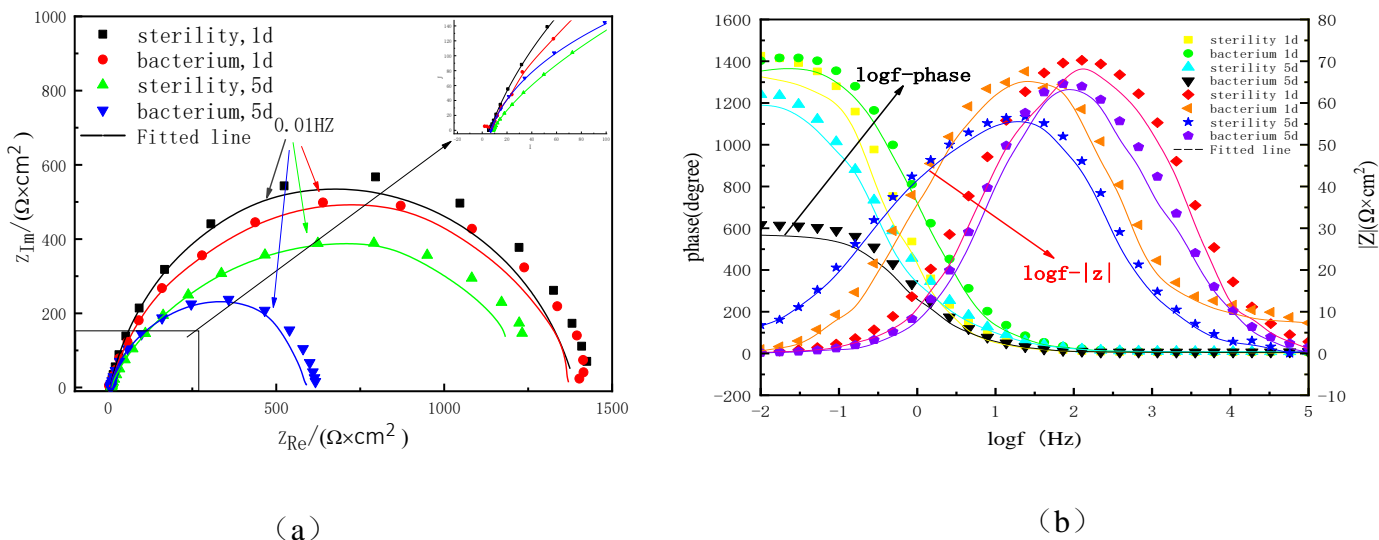


Figure 5. Electrochemical impedance spectroscopy of X80 steel in Dagang soil simulated solution under the bacterial and sterile conditions at self-corrosion potential (a) Nyquist diagram (b) Bode diagram

The equivalent circuit $R (C (R (CR)))$ was used to fit the AC impedance diagram. The fitting circuit diagram is shown in Figure 6. And the $R_p = R_t + R_f$. As can be seen from the diagram, the experimental data was in good agreement with the fitting curve. C_{dl} represents electric double layer

capacitance, R_s represents the solution resistance in the reaction process, R_t represents the charge transfer resistance in the reaction process, R_f represents the the film resistance of the corrosion products generated, and R_p represents the polarization resistance in the whole reaction process, defining $R_p = R_t + R_f$. The polarization resistance can represent the resistance of the electrochemical reaction. The value of R_p^{-1} is proportional to the corrosion rate of the metal. The higher the R_p^{-1} , the faster the corrosion rate of the metal. The change of R_p value under different conditions without applied potential is shown in Figure 7. It can be seen that under the same soaking time, the R_p value fitted in the simulated solution with SRB was lower than that in the sterile Dagang simulated solution, indicating that the biofilm could obvious promote metal corrosion at this time. R_p value changes as follows: bacterium 5d < sterility 5d < bacterium 1d < sterility 1d.

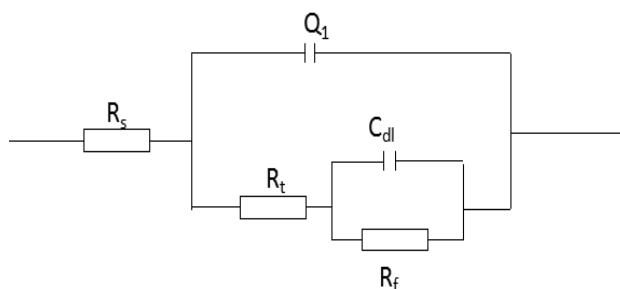


Figure 6. Equivalent circuit model of X80 steel in Dagang soil simulated solution under the bacterial and sterile conditions at self-corrosion potential

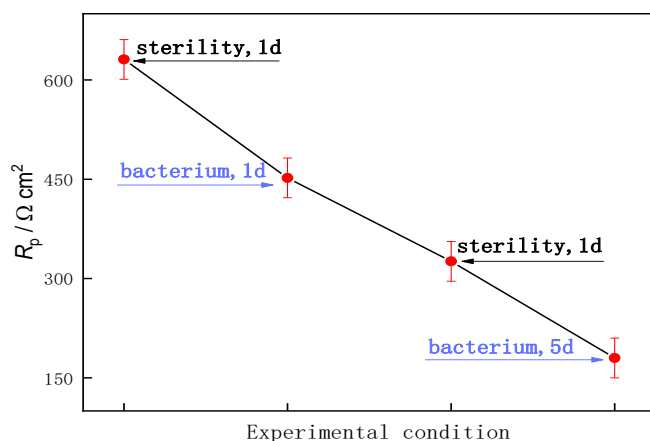


Figure 7. Equivalent circuit model of X80 steel in Dagang soil simulated solution under the bacterial and sterile conditions at self-corrosion potential

3.2 observation of corrosion morphology

The corrosion morphology of polarized metal surface under -800mV cathodic potential is shown in Figure 8. Figure 8 (a) showed the corrosion morphology of X80 steel after soaking in sterile Dagang soil simulated solution for 1 day. The degree of corrosion was mild, the traces of sanding paper could be

seen on the surface, and there were small pitting pits on the surface. Figure 8 (b) showed the corrosion morphology of X80 steel soaked in Dagang soil simulated solution with SRB for 1 day. There are obvious corrosion pits on the metal surface, and the corrosion degree was deeper than that of Figure (a). Figure 8 (c) showed the corrosion morphology of X80 steel soaked in sterile Dagang soil simulated solution for 5 days. The pitting pits on the metal surface are obvious and there are a large number of pitting pits, indicating that the corrosion degree deepens with the increase of time. Figure 8 (d) showed the corrosion morphology of X80 steel soaked in Dagang soil simulated solution with SRB for 5 days. At this time, the corrosion degree of metal surface was the most serious.

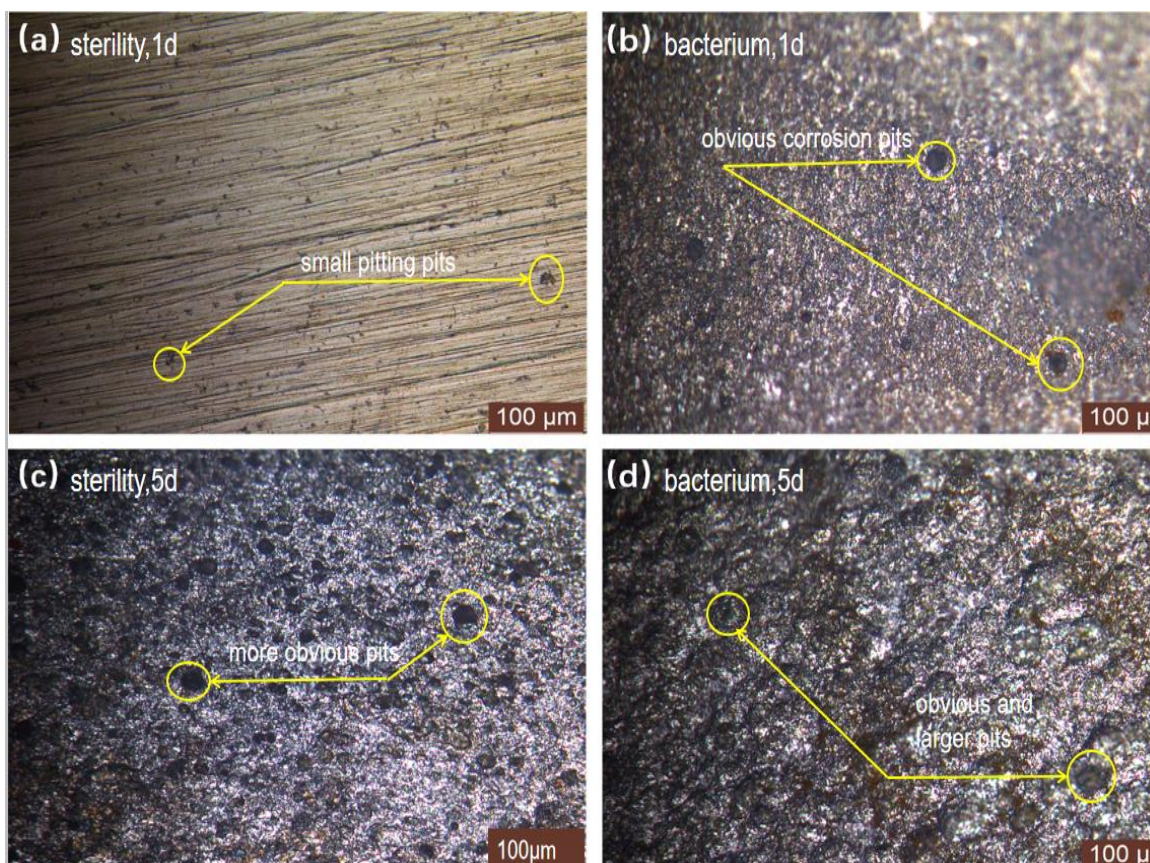


Figure 8. Corrosion morphology of X80 steel surface in Dagang soil simulated solution under the bacterial and sterile conditions at -800mV potential (a. sterility 1d; b. bacterium 1 d; c. sterility 5 d; d. bacterium 5 d)

The corrosion morphology of polarized metal surface without applied potential is shown in Figure 9. Figure 9 (a) showed the corrosion morphology of X80 steel soaked in sterile Dagang simulation solution for 1 day. Compared with Figure 9 (a), it can be found that the metal surface was more likely to be corroded without applied potential protection, but no obvious corrosion pit had been observed on the metal surface because of the short corrosion time. Figure 9 (b) showed the corrosion morphology of X80 steel soaked in Dagang soil simulated solution with SRB for 1 day. There were many tiny corrosion pits on the metal surface, and the corrosion degree was deeper than that of Figure 9 (a). Figure 9 (c) showed the corrosion morphology of X80 steel soaked in sterile Dagang soil simulated solution for 5 days. The

number of corrosion pits on the metal surface increased obviously, indicating that the degree of corrosion deepened with the increase of time. Figure 9 (d) showed the corrosion morphology of X80 steel soaked in Dagang soil simulated solution with SRB for 5 days. At this time, the corrosion pits on the metal surface were obviously added.

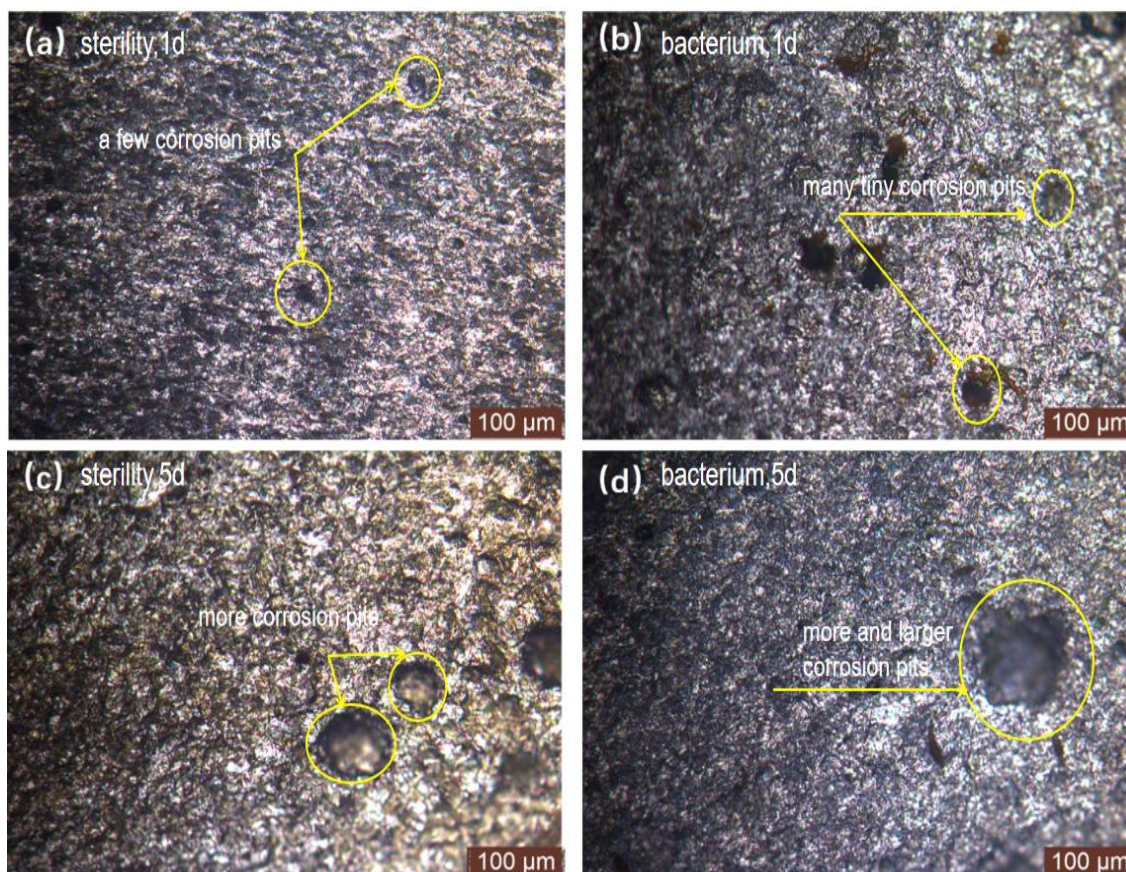


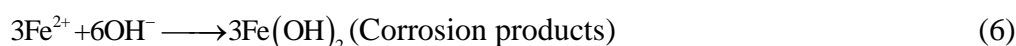
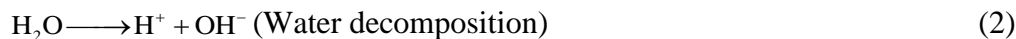
Figure 9. Corrosion morphology of X80 steel surface in Dagang soil simulated solution under the bacterial and sterile conditions at self-corrosion potential (a. sterility 1d; b. bacterium 1 d; c. sterility 5 d; d. bacterium 5 d)

3.3 discussion

3.3.1 Effect of applied cathodic potential on electrochemical corrosion of film forming X80 steel

At a certain applied potential, SRB is firstly adsorbed on the lattice defects such as vacancies and dislocations on the electrode surface of X80 pipeline steel.[23] This is due to the high surface energy and activity of the metal at the defects, which is easy to cause lattice distortion, and then the adsorption occurs.[24] With the metabolism of SRB, the extracellular polymeric substances (EPS) with certain strength and viscosity is generated, which is easily attached to the metal surface to form a biofilm with sulfate reducing bacteria cells. The biofilm coated on the metal surface can change the surface energy and corrosion potential of X80 pipeline steel, thus changing the electrochemical process of metal corrosion. With the progress of corrosion, the biofilm is uniformly covered on the metal surface, which

slows down the diffusion rate of oxygen to the metal surface, thus forming a low-oxygen zone nearby, where the air is not easily accessible under the biofilm as an anode, and around the anode is used as a cathode to form an oxygen concentration cell. Through the depolarization of the cathode, the sulfate reducing bacteria can oxidize the adsorbed hydrogen and accelerate the corrosion reaction of hydrogen evolution from the cathode.[25]The specific reaction process is shown in chemical formulas (1) to (7).[26]



At -800mv cathodic potential, the application of cathodic polarization potential can effectively inhibit the adhesion of biofilm. This is because when the applied potential is -800mv, the increase of cathodic current suppresses the electron transfer process, the cathodic depolarization of SRB is weakened, and the sample is in the state of cathodic protection. Saravia et al studied the effects of common desulphurization vibrio, desulphurization vibrio and vibrio alginolyticus on 304L stainless steel when cathodic protection was applied, and concluded that when cathodic protection was applied at the initial stage of biofilm growth, the amount of bacterial adsorption decreased significantly, while when cathodic protection was applied after the biofilm was formed, the amount of bacterial adsorption did not decrease. [27] Dongju Sun et al pointed out that the cathodic polarization of proper potential on the electrode surface can effectively inhibit the adhesion of biofilm, in which the polarization potential which can effectively inhibit the biofilm adhesion on the surface of stainless steel is within the potential range of cathodic protection, so the selection of appropriate polarization potential can play the role of cathodic protection and biological antifouling at the same time. [28] This is consistent with the conclusion of this experiment.

3.3.2 Corrosion mechanism of SRB on X80 steel under applied cathodic potential

In the process of electrochemical corrosion, the electrons lost by Fe can only be transferred to SRB with the help of electron transfer medium. H can be used as a medium for indirect electron transfer between SRB and polarized electrode. H⁺ moves towards the electrode surface and is reduced to [H] on the electrode surface; [H] reduces SO₄²⁻ under the catalysis of hydrogenase in SRB and provides a certain amount of energy for the metabolism of SRB, thus promoting the growth and metabolism of SRB, and then affecting the electrochemical corrosion of metals [29]. The mechanism of corrosion process in Dagang soil simulated solution is shown in Figure 10.

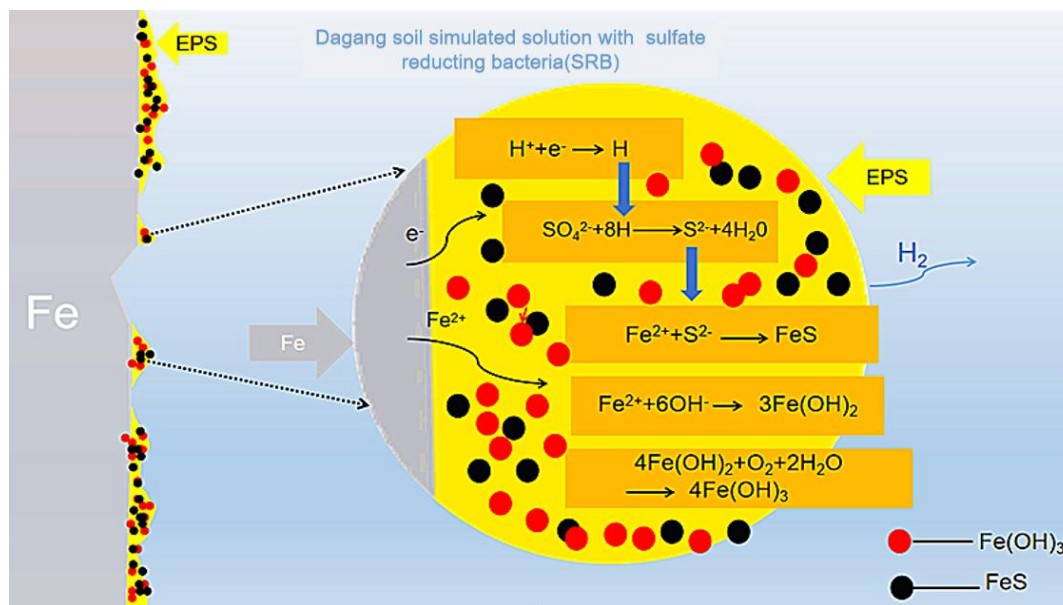


Figure 14. The mechanism of corrosion process for X80 steel in Dagang soil simulated solution with SRB

Under the applied potential, the electrochemical corrosion rate of metals decreases obviously. This may be due to the decrease of the rate of H^+ moving to the electrode surface after the application of cathodic potential. Studies have shown that the applied protection potential will decrease by 0.1V in the presence of active SRB. [30]Some research results even show that due to the change of metal corrosion potential caused by cathodic polarization, the cathodic polarization potential in sterile environment becomes anodic polarization in environment with SRB, that is, the open circuit potential of metal in SRB medium is more negative than the best cathodic protection potential in sterile environment.[31]Qingmiao Ding studied the applicability of the cathodic protection criterion of X80 steel in seawater solution containing SRB by surface observation and electrochemical method, and concluded that cathodic protection can play a cathodic polarization effect on X80 steel in seawater solution environment with SRB[32]By studying the influence of polarization potential on the electrochemical behavior of X70 steel in the marine environment containing SRB, Xu Chen found that when there was no applied potential, the growth cycle of SRB in marine environment could be divided into three stages: logarithmic growth period, stable growth period and decay period, and the number of SRB reached the maximum from day 6 to day 9. Under the stimulation of applied cathodic electric field, the mitotic cycle of SRB was shortened and the rate of cell division was increased, thus promoting the reproduction of SRB. However, the cathodic electric field also accelerated the death of SRB.[33]The above scholars' conclusion proves that the growth cycle of SRB will be affected under the applied potential, thus changing the corrosion rate of X80 steel. This is consistent with the conclusion of this experiment.

4. CONCLUSIONS

(1) In Dagang soil simulated solution, the anode of X80 pipeline steel shows typical activation control. In the environment of - 800mv cathode potential, the electrochemical corrosion rate of X80 pipeline steel is obviously reduced, and the corrosion rate is gradually accelerated with the increase of soaking time.

(2) The electrochemical corrosion rate of X80 steel measured in sterile Dagang soil simulated solution is lower than that in the simulated solution with SRB. Sulphate reducing bacteria play an obvious role in promoting the corrosion of X80 pipeline steel.

ACKNOWLEDGMENTS

This work was supported by Liaoning Natural Science Foundation Guidance Program: (Grant No. 20180550669) and Liao Ning Revitalization Talents Program: (Grant No. XLYC1807260).

References

1. M. Zhou, L. X. Du, Y. F. Zhao, X. H. Liu, *Journal of Wuhan University of Technology - Mater Sci Ed*, 27 (2012) 252.
2. M.T. Wang, Y. He, L. Wang, L. Z. Su, D. M. Niu, G. Z. Li, *Welder*, 39 (2009) 6.
3. C. Chen, J. J. Wu, *Mid-month talk*, 12 (2016) 45.
4. C. M. Xu, Y. H. Zhang, G. X. Cheng, W. S. Zhu, C. Chen, J. J. Wu, *J. Mater. Sci. Eng*, 6 (2006) 23
5. X. G. Li, D. W. Zhang, Z. Y. Liu, Z. Liu, C. W. Du, C. F. Dong, *Nature*, 527 (2015) 441.
6. F. M. Alabbas, C. W. Williamson, S. M. Bhola, J. R. Spear, D. L. Olson, B. Mishra, A. E. Kakapovbia, *J. Mater. Eng. Perform.*, 22 (2013) 3517.
7. R. Javaherdashti, *Appl. Microbiol. Biotechnol.*, 91 (2011) 1507.
8. J. Wang, Q. Li, M. M. Li, T. H. Chen, Y. F. Zhou, Z. B. Yue, *Bioresour. Technol.*, 163 (2014) 374.
9. Z. H. Dong, T. Liu, H. F. Liu, *Biofouling*, 27 (2011) 487.
10. H. H. P. Fang, L. C. Xu, K. Y. Chan, *Water Res.*, 36 (2002) 4709.
11. S. D. Silva, R. Basséguy, A. Bergel, *Electroanal. Chem.*, 561 (2004) 93.
12. Z. Y. Liu, X. G. Li, Y. F. Chang, *Corros. Sci.*, 55 (2012) 54.
13. Z. Y. Liu, X. G. Li, C. W. Du, G. L. Zhai, Y. F. Cheng, *Corros. Sci.*, 50 (2008) 2251.
14. J. L. Zhou, X. G. Li, C. W. Du, Y. L. Li, T. Li, *Acta Metall. Sinica*, 46 (2010) 251.
15. J. Q. Wang, A. Atrens, *Corros. Sci.*, 45 (2003) 2199.
16. B. Gu, J. L. Luo, X. Mao, *Corrosion*, 55 (1999) 312.
17. Y.F. Cheng, *Electrochim. Acta*, 52 (2007) 2661.
18. Z. Y. Liu, G. L. Zhai, X. G. Li, C. W. Du, *Journal of University of Science and Technology Beijing*, 15 (2008) 707.
19. P. Liang, C. W. Du, X. G. Li, X. Chen, L. Zhang, *Int. J. Miner. Metall. Mater.*, 4 (2009) 407.
20. X. Chen, C. W. Du, X. C. Li, P. Liang, X. R. Lu, *Journal of University of Science and Technology Beijing*, 30 (2008) 730.
21. C. Y. Chen, S. Xiang, Y. N. Hu, Y. Liang, W. Shi, *Acta Mater*, 30 (2016) 62.
22. C. M. Xu, Y. H. Zhang, G. X. Cheng, W. S. Zhu, *Journal of Chinese Society for Corrosion and Protection*, 27 (2007) 48.
23. J. E. G. González1a, F. J. H. Santana1, J. C. Mirza-rosca2, *Corros. Sci.*, 40 (1998) 2141.
24. P. Angell, K. Urbanic, *Corros. Sci.*, 42 (2000) 897.
25. H. Castaneda, X. D. Benetton, *Corros. Sci.*, 50 (2008) 1169.

26. H. W. Liu, F. Cheng, *Electrochim. Acta*, 253 (2017) 368.
27. S. G. G. Saravia, M. F. L. Mele, H. A. Videla, *Biofouling*, 11 (1997) 1.
28. D. J. Sun, L. D. Wang, G. C. Liu, Y. Li, K. Y. Zhang, S. C. Hou, J. Zhang, H. J. Zhang, *Liaoning Chemical Industry*, 43 (2014) 980.
29. J. J. Li, Y. M. Liu, X. W. Zhang, H. K. Teng, S. F. Wang, *Industrial Water Treatment*, 27 (2007) 4.
30. F. Guan, X. F. Zhai, J. Z. Duan, B. R. Hou, *Journal of Chinese Society for Corrosion and Protection*, 38 (2018) 1.
31. D. K. Xu, T. Y. Gu, *Int. Biodeterior. Biodegrad.*, 91 (2014) 74.
32. Q. M. Ding, Y. M. Fan, Y. F. Zhang, *Journal of Marine Sciences*, 34 (2016) 19.
33. X. Chen, B. Wang, X. Y. Ren, W. J. Chen, M. Wu, D. J. Chen, C. H. Wang, *Corrosion Science and Protection Technology*, 30 (2018) 343.

© 2020 The Authors. Published by ESG (www.electrochemsci.org). This article is an open access article distributed under the terms and conditions of the Creative Commons Attribution license (<http://creativecommons.org/licenses/by/4.0/>).